Macroscopic polarization entanglement and loophole-free Bell inequality test

M. Stobińska,[1,2,*] P. Horodecki,[3,4] A. Buraczewski,[5]
R. W. Chhajlany,[3,4,6] R. Horodecki,[4,7] and G. Leuchs[2,8]

[1]*Institute for Theoretical Physics II, Erlangen-Nürnberg University, Erlangen, Germany*

[2]*Max Planck Institute for the Science of Light, Erlangen, Germany*

[3]*Faculty of Applied Physics and Mathematics, Gdańsk University of Technology, Gdańsk, Poland*

[4]*National Quantum Information Center of Gdańsk, Sopot, Poland*

[5]*Faculty of Electronics and Information Technology, Warsaw University of Technology, Warsaw, Poland*

[6]*Faculty of Physics, Adam Mickiewicz University, Poznań, Poland*

[7]*Institute of Theoretical Physics and Astrophysics, University of Gdańsk, Gdańsk, Poland*

[8]*Institute for Optics, Information and Photonics, Erlangen-Nürnberg University, Erlangen, Germany*

Quantum entanglement [1, 2] revealed the inconsistency between the classical and the quantum laws governing the living and inanimate matter [3, 4]. Quantum mechanical predictions contradict local realistic theories [1] leading to a violation of Bell inequalities [5, 6] by entangled states. All experiments confirming the violation suffered from loopholes [7–10], a fundamental problem in modern physics [11–13]. Detection loopholes result from data postselection due to inefficient photodetection of single quanta. Large quantum systems though difficult to produce, bring us closer to complex biological organisms allowing for testing their quantum nature [14–17]. Here we show that loophole-free Bell tests are possible within the current technology using multi-photon entanglement [18] and linear optics. A preselection protocol prepares the macroscopic in photon

*Electronic address: magda.stobinska@mpl.mpg.de

number entanglement (10^3 photons at least) in advance, making the postselection unnecessary. Complete loss of the state is impossible and dark counts are negligible. Fast switching measurements close the locality loophole. Macroscopic preselected states find application in creating quantum superpositions of living organisms and their manipulation [15].

The multi-photon polarization entanglement has recently been demonstrated [18–20]. First, a two–mode pair of linearly polarized photons is created in a standard singlet through parametric down conversion (PDC). We describe the PDC process in terms of polarization states lying in the equatorial plane, $|1_\varphi\rangle = 1/\sqrt{2}(|1_H, 0_V\rangle + e^{i\varphi}|0_H, 1_V\rangle)$ and its orthogonal counterpart $|1_{\varphi^\perp}\rangle$, parametrized by the polar angle φ, where $|n_H, m_V\rangle$ denotes n (m) photons polarized horizontally (vertically). The singlet takes the form

$$\frac{1}{\sqrt{2}}(|1_\varphi\rangle_A|1_{\varphi^\perp}\rangle_B - |1_{\varphi^\perp}\rangle_A|1_\varphi\rangle_B). \tag{1}$$

Next, the population of each PDC outcoming spatial mode (A and B) can be independently phase sensitive amplified to create a multi-photon state by passing the appropriate photon through an intensely pumped high gain g nonlinear medium. We denote amplified $|1_\varphi\rangle$ and $|1_{\varphi^\perp}\rangle$ multi-photon states for a fixed φ as $|\Phi\rangle$ and $|\Phi_\perp\rangle$, respectively. Those states reveal interesting interplay between polarization and photon number degrees of freedom: $|\Phi\rangle$ consists of all combinations of odd photon numbers $(1, 3, 5, ...)$ in φ and even photon numbers $(0, 2, 4, ...)$ in $\varphi^\perp$ polarization whereas $|\Phi_\perp\rangle$ consists of all combinations of even photon numbers in φ and odd photon numbers in $\varphi^\perp$ polarization (see Fig.1(a)). Due to different parity of photon numbers in φ and $\varphi^\perp$ polarizations these states are orthogonal. In the experiment, they contained up to $4m = 10^4$ photons on average, where $m = \mathrm{sh}^2 g$. However, small as well as large photon number components contribute to them. Amplification of one singlet mode e.g. B, leads to a "micro-macro" singlet $1/\sqrt{2}(|1_\varphi\rangle_A|\Phi_\perp\rangle_B - |1_{\varphi^\perp}\rangle_A|\Phi\rangle_B)$. If both modes were amplified, a "macro-macro" entangled state $1/\sqrt{2}(|\Phi\rangle_A|\Phi_\perp\rangle_B - |\Phi_\perp\rangle_A|\Phi\rangle_B)$ would be produced. The Bell test with these singlets would not be practical since multi-photon states $|\Phi\rangle$ and $|\Phi_\perp\rangle$ have to be fully distinguishable. Although the probability distributions $Q_\Phi(n_\varphi, n_{\varphi^\perp}) = |\langle n_\varphi, n_{\varphi^\perp}|\Phi\rangle|^2$ and $Q_{\Phi_\perp}(n_\varphi, n_{\varphi^\perp})$ do not overlap on the single photon scale (see Fig.3(a) and (b)) there are no detectors allowing parity measurements for intense beams. An effective overlap (resulting from small photon numbers) of order of 10^{-1} is measured as if Q–functions were continuous [18](see Fig.3(c)).

(a) (b)

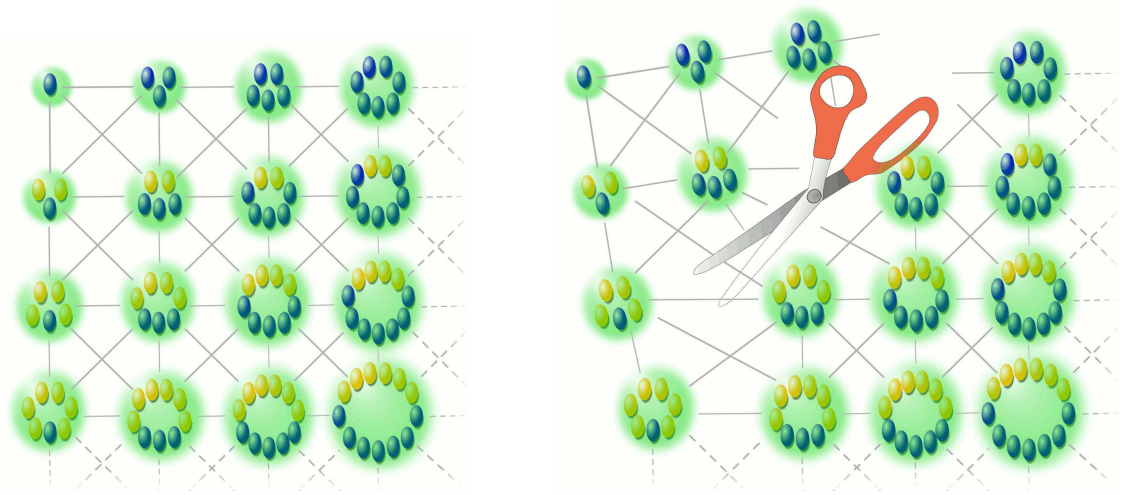

FIG. 1: (a) Multi-photon state $|\Phi\rangle$ consists of all combinations of odd photon numbers in φ (blue ellipses) and even photon numbers in $\varphi^{\perp}$ (yellow ellipses) polarization. (b) Quantum scissors (preselection protocol) cut-off the small photon numbers.

Our proposal does not rely on the orthogonality of the odd and even Fock states. Here, we propose a new preselection protocol which shifts the entanglement to high photon-numbers and makes the Q–functions unambiguously distinguishable for detection. It acts as quantum scissors which cut-off the small photon number contributions in multi-photon states and thus produce a genuine macroscopic state useful for a Bell test (see Fig.1(b)). It rejects states for which $n_{\varphi} + n_{\varphi^{\perp}} \leq N_{th}$ where N_{th} is a certain (approximate) threshold for the acceptable smallest number of photons in each preselected multi-photon state, see Fig. 2(a). The above condition imposes a constraint only on the sum of the two photon numbers but gives no information about the polarization components. After preselection the odd-even structure of the Q–functions is lost. Ideally, the process is carried out by the projector

$$\mathcal{P}_{n_{\varphi}+n_{\varphi^{\perp}}>N_{th}} \equiv \sum_{n_{\varphi},n_{\varphi^{\perp}}:n_{\varphi}+n_{\varphi^{\perp}}>N_{th}} |n_{\varphi}\rangle\langle n_{\varphi}| \otimes |n_{\varphi^{\perp}}\rangle\langle n_{\varphi^{\perp}}|. \tag{2}$$

This however cannot be perfectly implemented with current technology, though an arbitrarily good approximation may be obtained for high average photon numbers. If N_{th} is high enough, the preselected macroscopic entangled output state approaches a macroscopic singlet state.

We will focus on "macro-macro" entanglement, though the argument is adoptable to the

"micro-macro" case.

Each multi-photon state from a multi-photon polarization entanglement source is passed through a preselecting unbalanced beamsplitter with a small reflectivity R, e.g. $R = 10\%$ and the reflected beam intensity is measured. The transmitted beam is accepted for Bell test if the number of reflected photons is greater than an appropriately chosen threshold K_{th}, Fig. 2(b). A large reflected intensity k means that a very large number, at least N_{th}, of photons are transmitted in the process given the strong bias of the beamsplitter. Indeed, reflection of more than $2R = 20\%$ of the impinging photons has negligible probability, implying that at least 80% of the photons must have been transmitted. To get a lower bound on the number of transmitted photons n, we assume the reflected number of photons to constitute the mentioned 20% of input photons and hence infer from the measured intensity $k \geq K_{th}$ (or $k < K_{th}$) if $n \geq N_{th}$ (or $n < N_{th}$). The transmitted beam is not in pure state for an arbitrary K_{th} (since a beamsplitter entangles reflected and transmitted beams) however, it is approximately in pure (projected) state for large K_{th}. The scheme works well for highly populated input states. The Q-functions for the preselected macroscopic states with $m = 10^3$ and $K_{th} = 1700$ obtained with the probability of success $p = 2 \cdot 10^{-3}$ are presented in Fig. 3(b). They are practically disjoint with overlap equal to $8 \cdot 10^{-5}$. In principle, one could preselect multi-photon states with a smaller photon number but the probability drops dramatically.

After successful preselection in both modes, the output entangled state can be used for a Bell test. The test with macroscopic singlets is highly desirable, as the probability of losing the state is negligible and dark counts are easy to notice. Similarly, small single photon detection efficiency is not a limiting factor even for a preselected "micro-macro" entangled state [21]. One may choose the basic observable in the form of a three-output intensity measurement

$$\mathcal{A}(\varphi) = \mathcal{P}_{n_\varphi \leq N_\sigma} \otimes \mathcal{P}_{n_{\varphi^\perp} > N_\sigma} - \mathcal{P}_{n_\varphi > N_\sigma} \otimes \mathcal{P}_{n_{\varphi^\perp} \leq N_\sigma}. \tag{3}$$

The eigenvalue -1(+1) corresponds approximately to a measurement of preselected state $|\Phi\rangle(|\Phi_\perp\rangle)$, *i.e.* the upper (lower) off–diagonal quadratures in Fig.3(b). The observable suggests the proper value of the N_σ parameter, which can be set at the detectors, for the examined preselected states for a given $K_{\rm th}$. It allows to maximally profit from the disjointness of the preselected states while minimizing the discarded part of the Q–functions. This feature weighs heavily on the correlation between the two macroscopic states. In short, N_σ defines the maximal number of $\varphi^\perp$ (φ) - polarized photons in the preselected

(a)

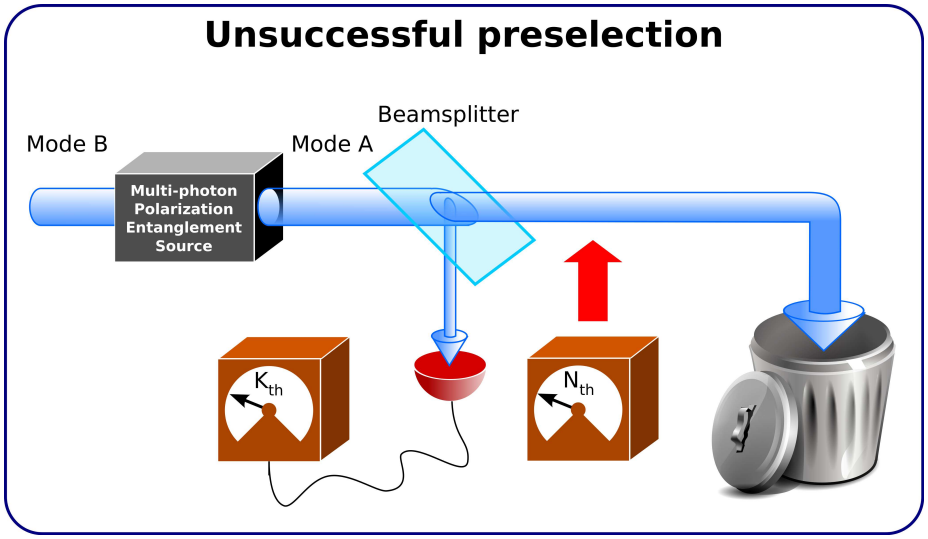

(b)

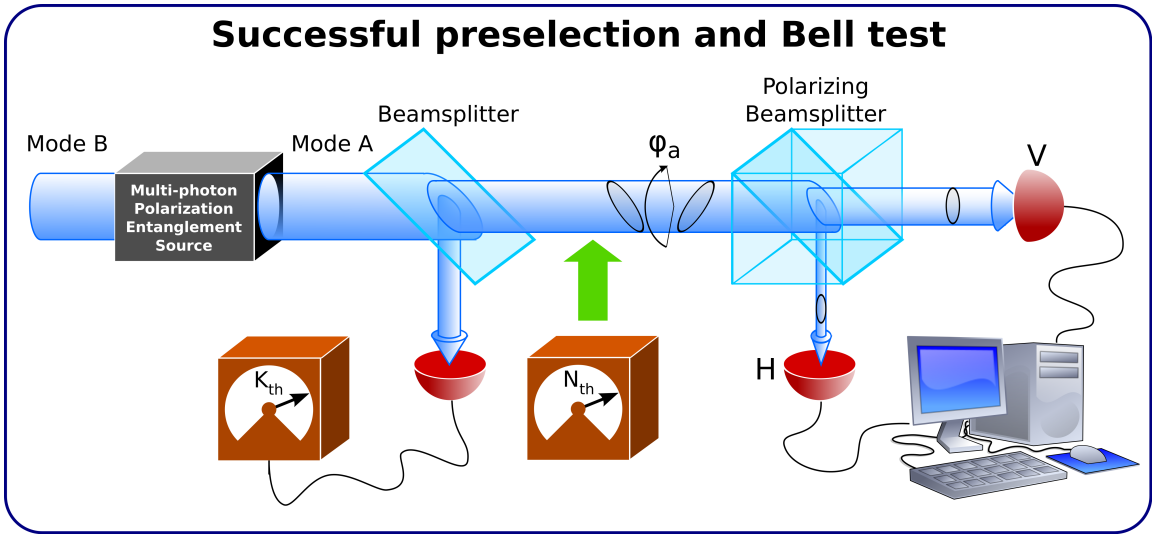

FIG. 2: The schematic for conditional preselection protocol (only mode A is shown). A multi-photon polarization entanglement source is followed by beamsplitters BS, phaseshifters PS and polarizing beamsplitters PBS. The Bell test is performed using preselected "macro-macro" polarization singlet only if the detectors measuring the reflected beams report photon numbers greater than the threshold K_{th} (b). Otherwise the state is rejected (a).

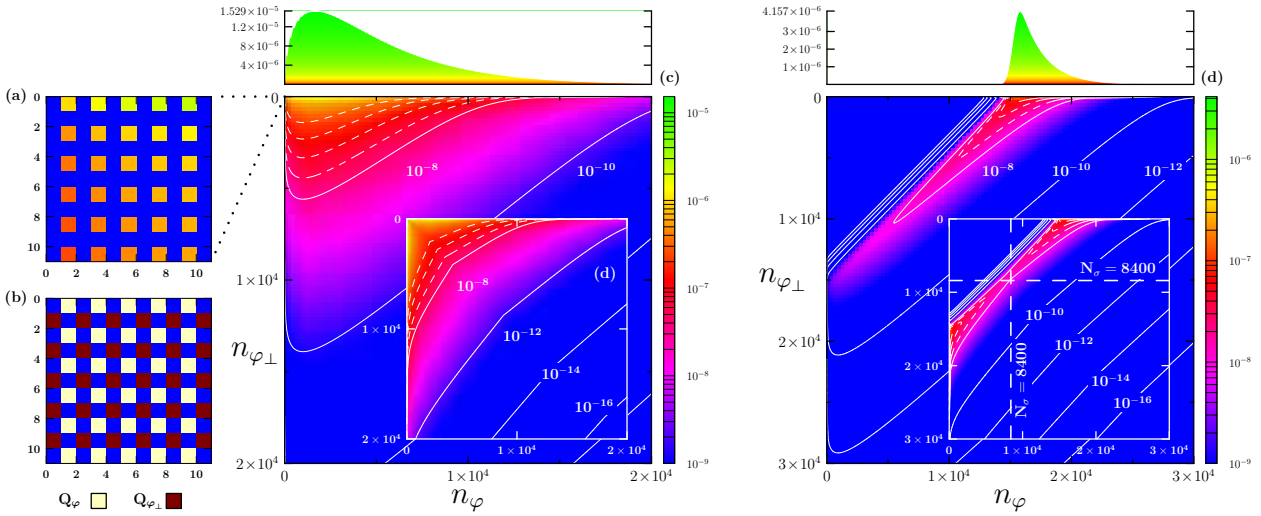

FIG. 3: The $Q_\Phi(n_\varphi, n_{\varphi^\perp})$ and $Q_{\Phi_\perp}(n_\varphi, n_{\varphi^\perp})$ distributions for $|\Phi\rangle$ and $|\Phi_\perp\rangle$ with $m = 10^3$, respectively. (a) before preselection Q_Φ is discrete on the single photon scale but (c) continuous on the macroscopic scale of detection. (b) the distributions Q_Φ and $Q_{\Phi_\perp}$ do not overlap on the single photon scale however, (d) huge effective overlap is measured. (e) Q_Φ is shifted to high photon number region after preselection with threshold $K_{th} = 1700$. (f) the distributions Q_Φ and $Q_{\Phi_\perp}$ for the same threshold. Q_Φ ($Q_{\Phi_\perp}$) is highly concentrated around the n_φ ($n_{\varphi^\perp}$) axis with a shadow constrained approximately within the regions $\{n_{\varphi^\perp} \leq N_\sigma,\ n_\varphi > N_\sigma\}$ ($\{n_\varphi \leq N_\sigma,\ n_{\varphi^\perp} > N_\sigma\}$), where $N_\sigma = 8400$.

states. For the considered case $N_\sigma = 8400$. The observable also accounts for violation of the filtering condition (measurement of either of the two diagonal quadratures in Fig.3(b)) due to imperfections in the preselection process yielding 0 in such circumstances. These results are inconclusive for Bell test and they contribute to the loophole (see Methods). Alternatively, one may choose a binary observable on only one of the polarization modes of preselected state

$$\bar{\mathcal{A}}(\varphi) = [\mathcal{P}_{n_\varphi < N_\sigma} - \mathcal{P}_{n_\varphi \geq N_\sigma}] \otimes I. \tag{4}$$

The Bell test is carried out using a Bell-CHSH observable

$$\begin{aligned} \mathcal{B} \ &= \ \mathcal{O}(\varphi_a) \otimes \mathcal{O}(\varphi_b) + \mathcal{O}(\varphi_a) \otimes \mathcal{O}(\varphi_{b'}) \\ &+ \ \mathcal{O}(\varphi_{a'}) \otimes \mathcal{O}(\varphi_b) - \mathcal{O}(\varphi_{a'}) \otimes \mathcal{O}(\varphi_{b'}), \end{aligned} \tag{5}$$

where $\mathcal{O}(\varphi) = \mathcal{A}(\varphi), \bar{\mathcal{A}}(\varphi)$ depending on the choice of the basic observable. Observable $\mathcal{O}$

is measured in the following steps: (i) the polarization of each macroscopic state is first independently rotated about the axis perpendicular to the equatorial plane of polarization through the angle φ using a Babinet-Soleil phase shifter (PS), (ii) followed by intensity measurements of the two reference polarization modes $\varphi = 0, \pi$. The angles are chosen as $\varphi_a = 0$, $\varphi_{a'} = \frac{\pi}{4}$, $\varphi_b = \frac{\pi}{8}$, $\varphi_{b'} = \frac{3}{8}\pi$. Bell inequality violation corresponds to $2 < |\langle \mathcal{B} \rangle| \leq 2\sqrt{2}$.

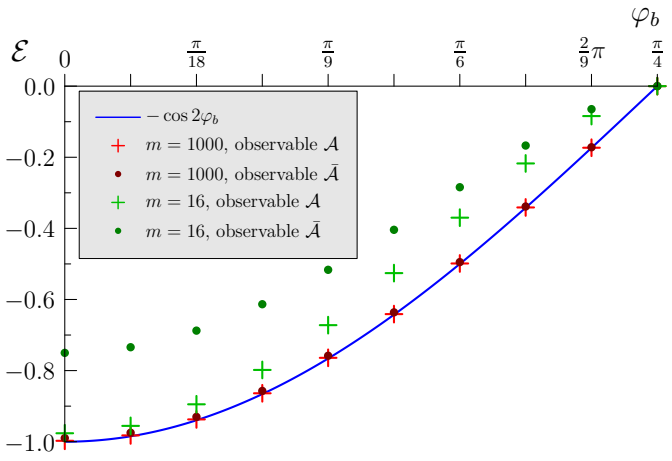

FIG. 4: Correlation function $\mathcal{E} = \langle \mathcal{O}(0) \otimes \mathcal{O}(\varphi_b) \rangle$ evaluated for preselected "macro-macro" singlet with $m = 16$ and $K_{th} = 70$ – green points and $m = 10^3$ and $K_{th} = 1700$ – red points.

The correlations $\langle \mathcal{O}(0) \otimes \mathcal{O}(\varphi_b) \rangle$ for states with mean number of photons $m = 16$ with $K_{th} = 70$ and $m = 10^3$ with $K_{th} = 1700$ are depicted in Fig.4. For $m = 10^3$ and perfectly aligned observables, $\langle \mathcal{O}(0) \otimes \mathcal{O}(\varphi_b) \rangle = -1$ revealing perfect singlet-like correlations in the state. However, for $m = 16$ observable $\bar{\mathcal{A}}(\varphi)$ reveals worse correlation than $\mathcal{A}(\varphi)$. Further testimony to the quality of state is provided by recalling that the angular dependence of the correlation in a singlet is given by $(-\cos 2\varphi_b)$. This dependence characterizes the preselected state accurately with rise in the mean number of photons. Also discrepancy between the values of the two observables decreases. For parameters shown in Fig.3, the best and almost maximal Bell inequality violation $\langle \mathcal{B} \rangle_{\mathcal{A}} = -2.82$ and $\langle \mathcal{B} \rangle_{\bar{\mathcal{A}}} = -2.80$ is indeed obtained for $N_\sigma = 8400$ for both observables with probability $p^2 = 3.9 \times 10^{-6}$. The observable $\mathcal{A}$ becomes loophole-free $\mathcal{L} = 0.003$. The results corresponding to $\bar{\mathcal{A}}$ are less perfect since it better witnesses deviations of the input state correlations from the singlet-like. The differences in results become more pronounced and lead to contradicting conclusions for non-optimal thresholds. Higher probability rates for the Bell inequality violation can be achieved for

lower values of thresholds e.g. p^2=1.7 $\times$ 10^{-3} is obtained for K_{th}=1000 and $N_\sigma = 5200$. In this case $\langle \mathcal{B} \rangle_{\mathcal{A}}$=−2.78 with $\mathcal{L}$=0.02 and $\langle \mathcal{B} \rangle_{\bar{\mathcal{A}}}$=−2.65 is obtained. In principle, Bell inequality violation is possible even for $m = 16$ however, it is not practical due to low probability of success. For further details see Methods section.

Importantly, our analysis shows that the scheme will work even in presence of losses or equivalently inefficient preselection. The detectors measure the threshold value K_{th}^{meas} with some uncertainty, thus its value is usually known up to 150 photons. Therefore, our input state should be rather considered as a mixture of preselected macroscopic entangled states for $K_{th} \in \langle K_{th}^{meas}-150, K_{th}^{meas}+150 \rangle$ than a single state for a given K_{th}^{meas}. However, for large m the higher values of N_σ, the broader window of K_{th} for which the preselected state reveals near perfect correlations and Bell inequality violation for the fixed measurement settings. For example, for $N_\sigma \in \langle 8200, 8600 \rangle$ we have the window of $K_{th} \in \langle 1400, 2400 \rangle$. This means that mixedness of the input state will not destroy Bell inequality violation since every term in the mixture leads to violation for the same set of angles. Other imperfections caused by absorption or dephasing of photons in the transmitted beam are negligible at short distances.

Our results find immediate application for testing the quantum nature of biological systems. Preselected macroscopic states are useful for creation of quantum non-gaussian superpositions of position and momentum of optically trapped species in a cavity via teleportation protocols [15, 22]. Creation of virus-light "micro-macro" singlet state via entanglement swapping will allow for manipulations on virus degrees of freedom in the strong coupling limit. Alternatively, the measurement performed on the light beam my allow to trace the virus position in the cavity.

In conclusion, we have shown the preselected, conditionally generated macroscopic entanglement to be a powerful resource for loophole-free Bell inequality testing within the current technology. These results are a proof-of-principle of the accessibility of such resources in real experimental situations. They find application in interdisciplinary research on testing of the quantum nature of biological systems as well as could be useful for quantum teleportation, security verification in quantum cryptology, controlled experimental analysis of quantum-to-classical transition phenomena [23] and experimental Bell tests using detectors with various detection profiles such as human eyes [24].

Methods

(i) The multi-photon states resulting from single photon amplification are as follows

$$|1_{\varphi}\rangle \rightarrow |\Phi\rangle = \sum_{i,j=0}^{\infty} \gamma_{ij} |(2i+1)_{\varphi}, (2j)_{\varphi^{\perp}}\rangle, \tag{6}$$
$$|1_{\varphi^{\perp}}\rangle \rightarrow |\Phi_{\perp}\rangle = \sum_{i,j=0}^{\infty} \gamma_{ij} |(2j)_{\varphi}, (2i+1))_{\varphi^{\perp}}\rangle,$$

with $\gamma_{ij} = C^{-2}(-\frac{\Gamma}{2})^i(\frac{\Gamma}{2})^j \frac{\sqrt{(1+2i)!(2j)!}}{i!j!}$, $C = \cosh(g)$, $\Gamma = \tanh(g)$.

(ii) The beamsplitter (BS) operation $U_{BS}|0,N\rangle = \sum_{k=0}^{N} c_k^{(N)} |k, N-k\rangle$ leads to the following probability amplitudes $c_k^{(N)} = \binom{N}{k}^{1/2} (R^k (1-R)^{N-k})^{1/2}$ for reflection of k and transmitting of $N-k$ photons. The BS is polarization independent. The BS preselected multi-photon states are as follows

$$|\tilde{\Phi}\rangle_{tr} = \mathcal{N} \sum_{i,j=0}^{\infty} \gamma_{ij} \sum_{n=0}^{2i+1} \sum_{m=m^*}^{2j} c_n^{(2i+1)} c_m^{(2j)} |(n)_{\varphi}, (m)_{\varphi^{\perp}}\rangle_r$$
$$\otimes |(2i+1-n)_{\varphi}, (2j-m)_{\varphi^{\perp}}\rangle_t,$$
$$|\tilde{\Phi}_{\perp}\rangle_{tr} = \mathcal{N} \sum_{i,j=0}^{\infty} \gamma_{ij} \sum_{n=0}^{2j} \sum_{m=m^*}^{2i+1} c_n^{(2j)} c_m^{(2i+1)} |(n)_{\varphi}, (m)_{\varphi^{\perp}}\rangle_r$$
$$\otimes |(2j-n)_{\varphi}, (2i+1-m)_{\varphi^{\perp}}\rangle_t,$$

where r and t denote the reflected and transmitted beams respectively, the normalization constant equals $\mathcal{N} = \sum_{i,j=0}^{\infty} |\gamma_{ij}|^2 \sum_{n=0}^{2i+1} \sum_{m=m^*}^{2j} |c_n^{(2i+1)}||c_m^{(2j)}|^2$ and $m^* = \max(0, K_{th} - n)$. The preselected macroscopic density operators (after the measurement on the reflected beam) for the Bell test are obtained by tracing over the reflected beam $\hat{\rho}(\tilde{\Phi}) = \mathrm{Tr}_r\{|\tilde{\Phi}\rangle_{tr}\langle\tilde{\Phi}|\}$, $\hat{\rho}(\tilde{\Phi}_{\perp}) = \mathrm{Tr}_r\{|\tilde{\Phi}_{\perp}\rangle_{tr}\langle\tilde{\Phi}_{\perp}|\}$. The "macro-macro" singlet state is given by

$$\hat{\rho} = 1/2 \times \mathrm{Tr}_r \left\{ \left(|\tilde{\Phi}\rangle_{tr} |\tilde{\Phi}_{\perp}\rangle_{tr} - |\tilde{\Phi}_{\perp}\rangle_{tr} |\tilde{\Phi}\rangle_{tr} \right) \right.$$
$$\left. \otimes \left(\langle\tilde{\Phi}|_{tr} \langle\tilde{\Phi}_{\perp}|_{tr} - \langle\tilde{\Phi}_{\perp}|_{tr} \langle\tilde{\Phi}|_{tr} \right) \right\}.$$

(ii) Overlap $\int \sqrt{Q_{\varphi}(n_{\varphi}, n_{\varphi^{\perp}}) \cdot Q_{\varphi^{\perp}}(n_{\varphi}, n_{\varphi^{\perp}})} dn_{\varphi} dn_{\varphi^{\perp}}$ between discrete Q_{φ}– and $Q_{\varphi_{\perp}}$– functions before preselection was calculated for convolution of these functions with Gauss function.

(iii) The loophole observable is defined as

$$\mathcal{L} = \mathcal{P}_{n_{\varphi} < N_{\sigma}} \otimes \mathcal{P}_{n_{\varphi^{\perp}} < N_{\sigma}} + \mathcal{P}_{n_{\varphi} > N_{\sigma}} \otimes \mathcal{P}_{n_{\varphi^{\perp}} > N_{\sigma}}. \tag{7}$$

It additively quantifies the violation of the preselection condition corresponding to measurement of either of the two diagonal quadratures in Fig.3(b) where the discarded part of Q–functions is located.

(iv) The differences in results in the Bell test obtained with observables in Eq.(3) and (4) become more pronounced and lead to contradicting conclusions for non-optimal thresholds e.g. for $K_{\rm th}$=1700 and N_σ=6000, $\langle\mathcal{B}\rangle_{\mathcal{A}}$=−2.59 > 2 and $\langle\mathcal{B}\rangle_{\bar{\mathcal{A}}}$=−1.90 < 2.

(v) Table I collects values of the correlation function $\langle\mathcal{O}(0)\otimes\mathcal{O}(0)\rangle$, the Bell parameter $\langle\mathcal{B}\rangle$ and the loophole $\mathcal{L}$.

(vi) Numerical simulations were performed with custom software written in C++ and with use of Class Library for Numbers (CLN). CLN offers greater precision over standard floating point numbers.

Acknowledgments

We thank A. Aiello, A. Lvovsky, M. Horodecki, M. Pawłowski and P. Sekatski for discussions. This work was partially supported by UE IP projects QAP and SCALA, Ministry of Science and Higher Education Grant No. 2319/B/H03/2009/37 and 2619/B/H03/2010/38 and by the Foundation for Polish Science. Computation was performed in the TASK Center at the Gdańsk University of Technology.

[1] Einstein, A., Podolsky, B. & Rosen, N. Can quantum-mechanical description of reality be considered complete? *Phys. Rev.* **47**, 777-780 (1935).

[2] Schrödinger, E. The present situation in quantum mechanics. *Naturwissenschaften* **23**, 807-812; 823-828; 844-849 (1935).

[3] Gröblacher, S. et al An experimental test of non-local realism. *Nature* **446**, 871-875 (2007).

[4] Norsen, T. Local Causality and Completeness: Bell vs. Jarrett. *Foundations of Physics* **39**, 273-294 (2009).

[5] Bell, J. S. On the Einstein-Podolsky-Rosen paradox. *Physics* **1**, 195-200 (1965).

[6] Clauser, J. F., Horne, M. A., Shimony, A. & Holt, R. A. Proposed experiment to test local hiddenvariable theories. *Phys. Rev. Lett.* **23**, 880-884 (1969).

[7] Aspect, A., Grangier, P. & Roger, G. Experimental Realization of Einstein-Podolsky-Rosen-Bohm *Gedankenexperiment*: A New Violation of Bell's Inequalities. *Phys. Rev. Lett.* **49**, 91-94 (1982).

[8] Weihs, G., Jennewein, T., Simon, Ch., Weinfurter, H. & Zeilinger, A. Violation of Bell's Inequality under Strict Einstein Locality Conditions. *Phys. Rev. Lett.* **81**, 5039-5043 (1998).

[9] Rowe, M. A. et al Experimental violation of a Bell's inequality with efficient detection. *Nature* **409**, 791-794 (2001).

[10] Matsukevich, D. N., Maunz, P., Moehring, D. L., Olmschenk, S. & Monroe, C. Bell Inequality Violation with Two Remote Atomic Qubits. *Phys. Rev. Lett.* **100**, 150404-150407 (2008).

[11] García-Patrón, R. et al Proposal for a Loophole-Free Bell Test Using Homodyne Detection. *Phys. Rev. Lett.* **93**, 130409-130412 (2004).

[12] Cabello, A., Rodríguez, D., & Villanueva, I. Necessary and Sufficient Detection Efficiency for the Mermin Inequalities. *Phys. Rev. Lett.* **101**, 120402-120405 (2008).

[13] Vértesi, T., Pironio, S. & Brunner, N. Closing the Detection Loophole in Bell Experiments Using Qudits. *Phys. Rev. Lett.* **104**, 060401-060404 (2010).

[14] Arndt, M., Juffmann, T. & Vedral, V. Quantum Physics meets biology. *HFSP Journal* **3**, 386-400 (2009).

[15] Romero-Isart, O., Juan, M. L., Quidant, R. & Cirac, J. I. Toward Quantum Superposition of Living Organisms. *New J. Phys.* **12**, 033015-16 (2010).

[16] Sarovar, M., Ishizaki, A., Fleming, G. R. & Whaley K. B. Quantum entanglement in photosynthetic light-harvesting complexes. *Nature Physics* **6**, 462-467 (2010).

[17] Collini, E., Wong, C. Y., Wilk, K. E., Curmi, P. M. G., Brumer, P. & Scholes G. D. Coherently wired light-harvesting in photosynthetic marine algae at ambient temperature. *Nature* **463**, 644-647 (2010).

[18] De Martini, F., Sciarrino, F. & Vitelli, Ch. Entanglement Test on a Microscopic-Macroscopic System. *Phys. Rev. Lett.* **100**, 253601-253604 (2008).

[19] De Martini, F. Entanglement and Quantum Superposition of a Macroscopic-Macroscopic system. *Found. Phys.* doi:10.1007/s10701-010-9417-3.

[20] Iskhakov, T. , Chekhova, M. V. & Leuchs, G. Generation and Direct Detection of Broadband Mesoscopic Polarization-Squeezed Vacuum. *Phys. Rev. Lett.* **102**, 183602-183605 (2009).

[21] Brunner, N., Gisin, N., Scarani, V. & Simon C., Detection Loophole in Asymmetric Bell

Experiments. *Phys. Rev. Lett.* **98**, 220403-220406 (2007).

[22] Ashkin, A. & Dziedzic, J. M. Optical Trapping and Manipulation of Viruses and Bacteria. *Science* **235**, 1517-1520 (1987).

[23] Zurek, W. H. Quantum Darwinism. *Nature Physics* **5**, 181-188 (2009).

[24] Sekatski, P., Brunner, N., Branciard, C., Gisin, N., & Simon, C. Quantum experiments with human eyes as detectors based on cloning via stimulated emission. *Phys. Rev. Lett.* **103**, 113601-113604 (2009).

$K_{\rm th}$	$N_\sigma = 8200$			$N_\sigma = 8400$			$N_\sigma = 8600$			$N_\sigma = 8800$		
1600	−0.996	−2.816	0.004	−0.994	−2.810	0.006	−0.990	−2.801	0.010	−0.986	−2.788	0.014
	−0.983	−2.779	–	−0.974	−2.756	–	−0.961	−2.719	–	−0.943	−2.668	–
1700	−0.997	−2.819	0.003	−0.997	−2.821	0.003	−0.997	−2.820	0.003	−0.996	−2.816	0.004
	−0.987	−2.791	–	−0.990	−2.800	–	−0.988	−2.795	–	−0.982	−2.778	–
1800	−0.992	−2.807	0.008	−0.995	−2.815	0.005	−0.997	−2.821	0.003	−0.998	−2.824	0.002
	−0.970	−2.744	–	−0.982	−2.777	–	−0.989	−2.799	–	−0.993	−2.809	–
1900	−0.984	−2.784	0.016	−0.989	−2.798	0.011	−0.993	−2.809	0.007	−0.996	−2.817	0.004
	−0.938	−2.653	–	−0.957	−2.706	–	−0.972	−2.749	–	−0.984	−2.782	–
$K_{\rm th}$	$N_\sigma = 5200$			$N_\sigma = 5400$			$N_\sigma = 5600$			$N_\sigma = 5800$		
900	−0.973	−2.753	0.027	−0.964	−2.728	0.036	−0.952	−2.693	0.048	−0.936	−2.649	0.064
	−0.894	−2.529	–	−0.860	−2.434	–	−0.814	−2.301	–	−0.754	−2.132	–
1000	−0.984	−2.783	0.016	−0.983	−2.781	0.017	−0.980	−2.771	0.020	−0.973	−2.753	0.027
	−0.936	−2.648	–	−0.934	−2.642	–	−0.920	−2.603	–	−0.895	−2.532	–
1100	−0.979	−2.769	0.021	−0.984	−2.784	0.016	−0.987	−2.791	0.013	−0.987	−2.792	0.013
	−0.918	−2.595	–	−0.937	−2.651	–	−0.948	−2.681	–	−0.948	−2.683	–
1200	−0.965	−2.730	0.035	−0.974	−2.756	0.026	−0.981	−2.776	0.019	−0.986	−2.790	0.014
	−0.863	−2.442	–	−0.899	−2.542	–	−0.926	−2.619	–	−0.945	−2.674	–

TABLE I: The correlation function, the Bell parameter $\langle\mathcal{B}\rangle$ and loophole $\mathcal{L}$ computed for the preselected "macro-macro" singlet with $m = 10^3$ for selected K_{th} and N_σ using $\mathcal{A}(\varphi)$ – the upper row and using $\bar{\mathcal{A}}(\varphi)$ – the bottom row. The quantum character of a state is revealed by $2 < |\langle B\rangle| \leq 2\sqrt{2}$.